Electronic Supplementary Information (ESI)

Three electron channels toward two types of active sites in MoS_2@Pt nanosheets for hydrogen evolution

X. Y. Xu,[a,‡,*] X. F. Dong,[a,‡] Z. J. Bao,[a] R. Wang,[a] J. G. Hu[a,*] and H. B. Zeng[b,*]

[a]*College of Physics Science and Technology, Yangzhou University, Yangzhou 225002, China. *E-mail: jghu@yzu.edu.cn; xxy@yzu.edu.cn; Fax: +86 0514 87975467; Tel: +86 0514 87970587*

[b]*Institute of Optoelectronics & Nanomaterials, Nanjing University of Science and Technology, Nanjing 210094, China. *E-mail: zeng.haibo@njust.edu.cn.*

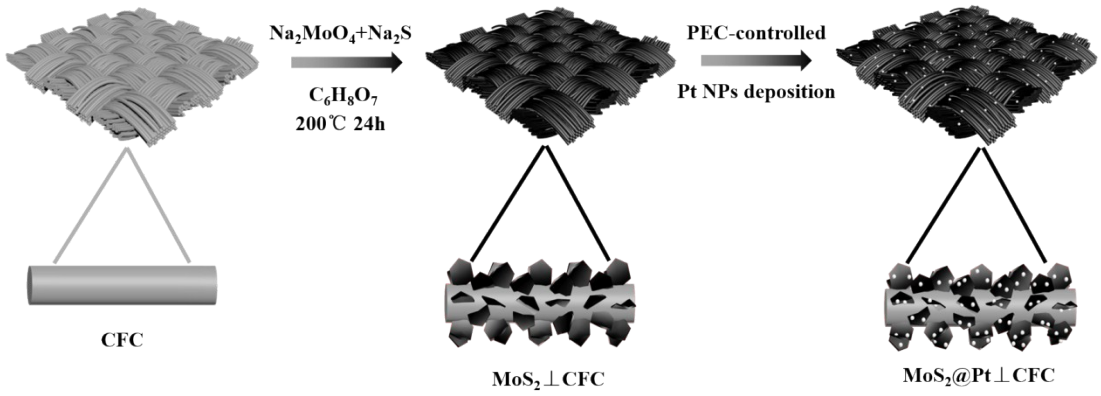

Fig. S1 Schematic illustration for synthesis processes of MoS_2/CFC and MoS_2@Pt/CFC electrodes. Vertically oriented MoS_2 NSAs were first grown around the washed CFC substrates via citric acid-assisted hydrothermal synthetic route with sodium molybdate and sodium sulfide as the Mo and S sources, respectively. After that, the time-dependent PEC control of in-situ deposition of Pt NPs on MoS_2 NSs was used to prepare the MoS_2@Pt catalysts with different loading of Pt NPs for different deposition time of 30, 60 and 90 min (MoS_2@Pt-1, MoS_2@Pt-2, and MoS_2@Pt-3).

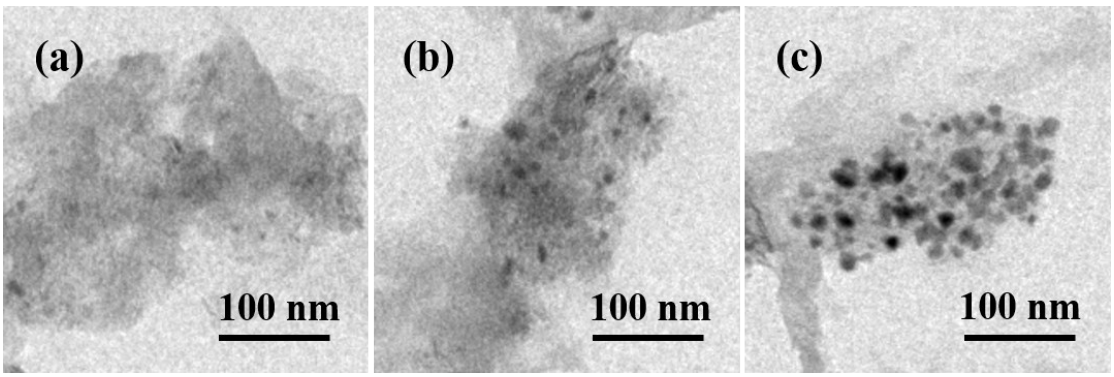

Fig. S2 TEM images of MoS_2 NSs after Pt decoration for different time of (a) 30, (b) 60 and (c) 90 min. The time-dependent PEC process was successfully used to control the in-situ deposition of Pt NPs on MoS_2 NSs. The MoS_2@Pt/CFC electrodes with different loading of Pt particles were obtained after the PEC treatment for different time of 30, 60 and 90 min, and labeled as MoS_2@Pt-1, MoS_2@Pt-2, and MoS_2@Pt-3, respectively.

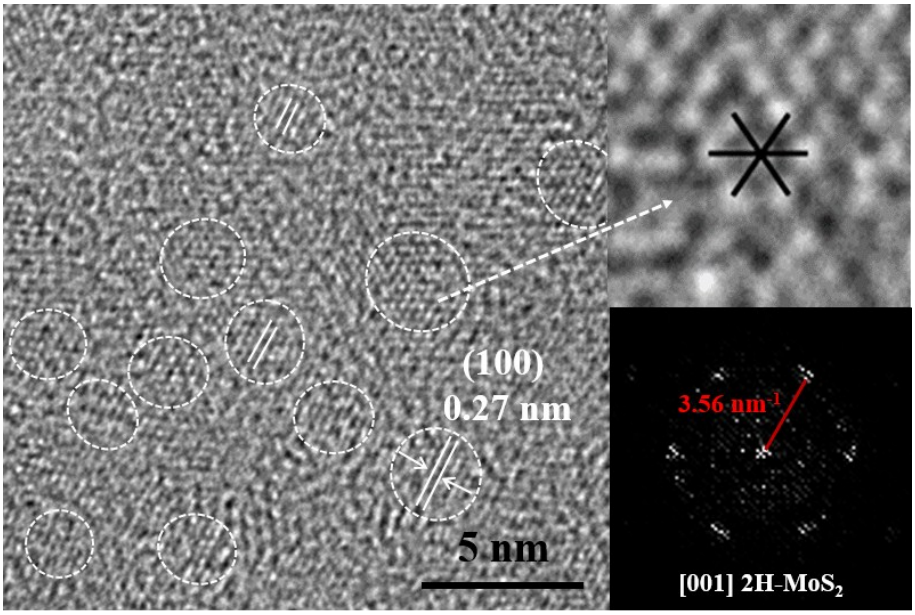

Fig. S3 Atomic resolution HRTEM image and corresponding FFT pattern for a typical ordering (100) domain. The honeycomb atom arrangement can be indexed to 2H-MoS_2.

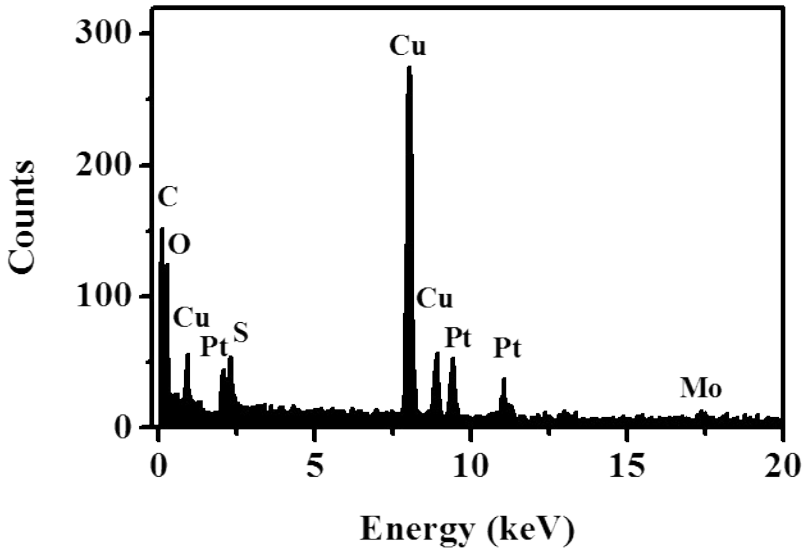

Fig. S4 EDX spectrum of typical MoS_2@Pt product. The composition of Mo, S and Pt elements in the MoS_2@Pt was determined, and the C and Cu elements come from the supporting base for TEM characterization.

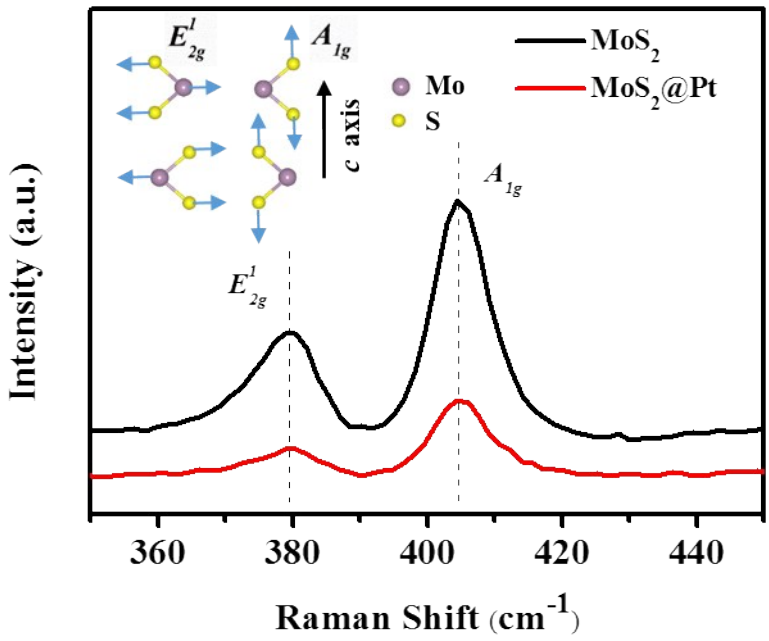

Fig. S5 Raman spectra of MoS_2 and MoS_2@Pt samples. Two characteristic peaks at around 379.1 and 404.4 cm^{-1} correspond to the in-plane E^1_{2g} mode, which is attributed to opposite vibration of two S atoms with respect to the Mo atom, and out-of-plane A_{1g} mode, which is associated with only S atom vibration in opposite directions.

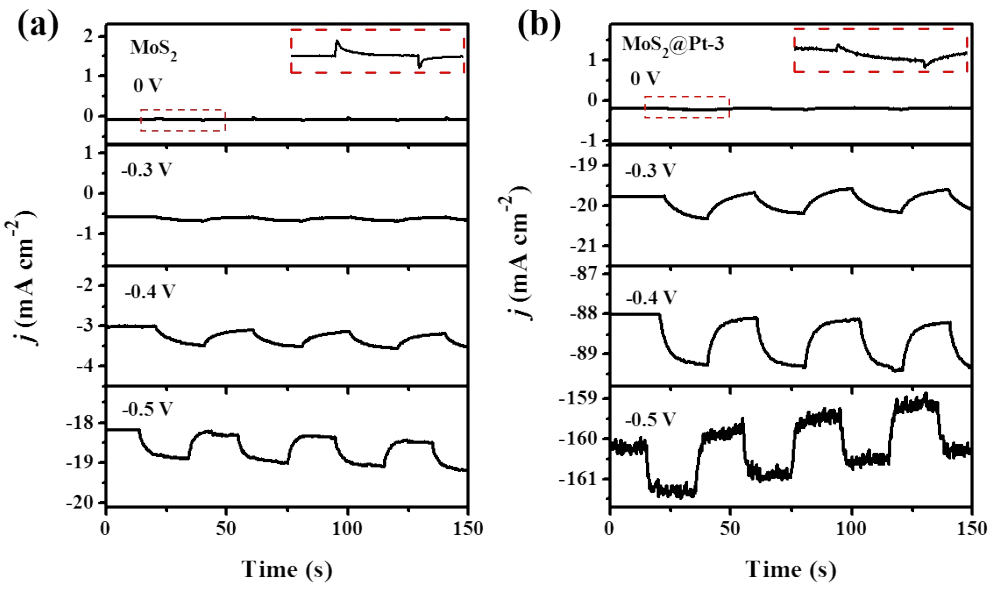

Fig. S6 Chronoamperometry ($j-t$) response under ON/OFF switched light irradiation for MoS_2 and MoS_2@Pt-3 electrodes in 0.5 M H_2SO_4 electrolyte at typical applied potentials of 0, -0.3, -0.4 and -0.5 V vs. SAE. The surface Pt decoration can remarkably improve the photocurrent response at any one potential and particularly make Δj_{light} faster grow to saturation over -0.4 V vs. SAE.

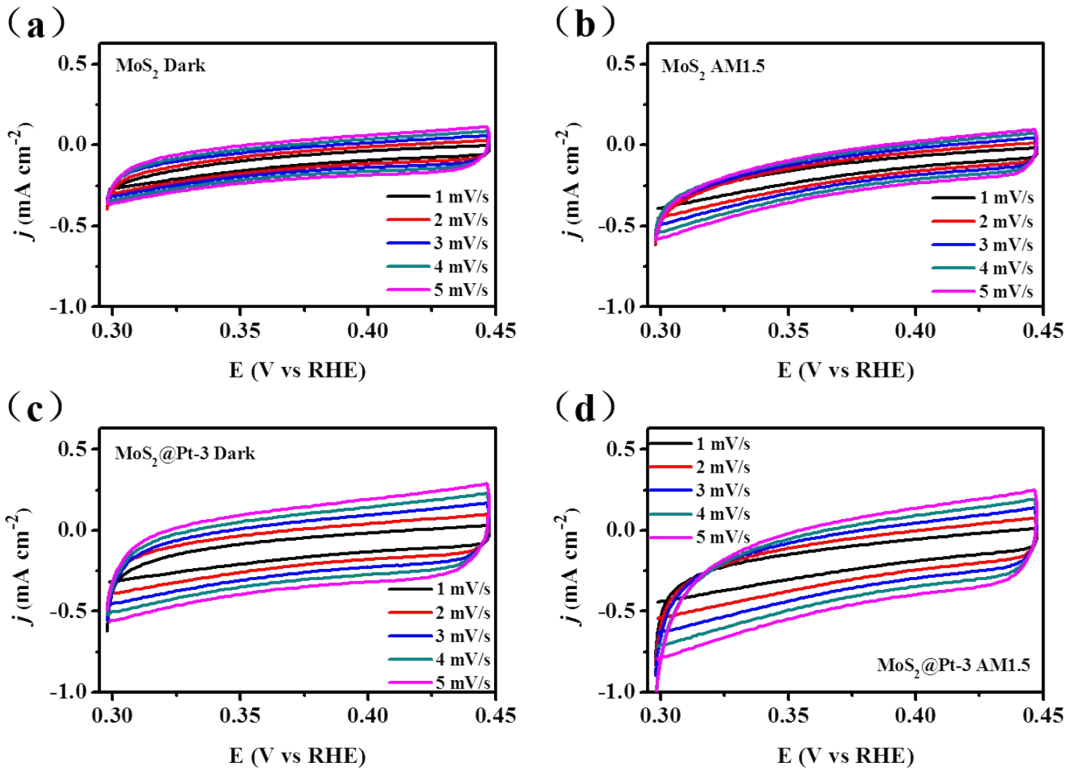

Fig. S7 CV curves of (a, b) MoS_2 and (c, d) MoS_2@Pt-3 electrodes in dark and light fields at different potential scanning rates. The scan rates are 1, 2, 3, 4 and 5 mV s^{-1}. The selected potential range where no faradic current was observed is 0.29 to 0.44 V vs. RHE. The halves of the positive and negative current density differences at the center of the scanning potential ranges were plotted versus the voltage scan rate to determine their EDLCs.

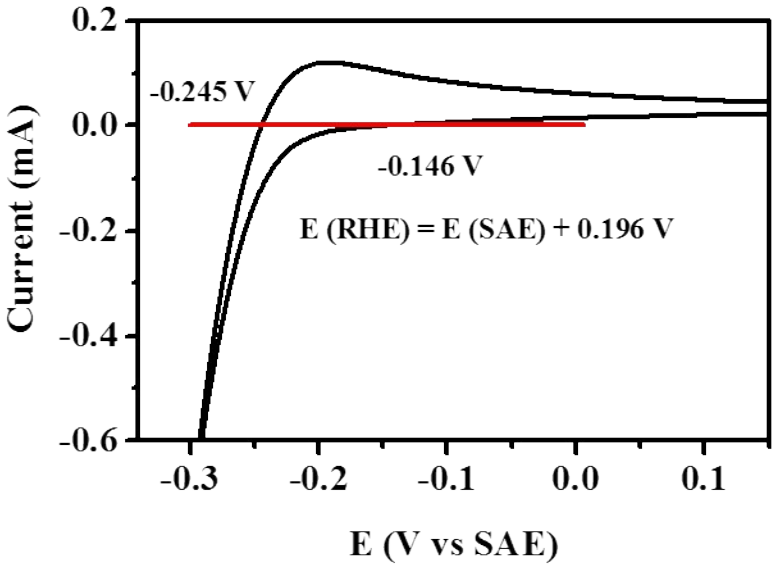

Fig. S8 CV curve for the potential calibration of SAE against RHE.

Table S1 Element proportion analysis for MoS_2@Pt product based on XPS data.

Name	Area(P) CPS.eV	Atomic %	Weight %
C 1s	271752.58	64.02	37.07
O 1s	188727.06	17.52	13.51
Mo 3d	292795.71	6.12	28.89
S 2p	101659.46	12.08	18.68
Pt 4f	20077.60	0.26	2.45

Table S2 Summary of literatures on electrocatalytic HER parameters of various MoS_2-based catalysts.

Catalyst	Electrolyte	Onset potention (mV vs RHE)	Over potential (mV vs RHE)	Exchange Current density (j_0, mA cm^{-2})*	Tafel slope (mV per decade)	Reference
Defect-rich MoS_2	0.5 M H_2SO_4	120	190	8.91×10^{-3}	50	1
Oxygen-incorporated MoS_2	0.5 M H_2SO_4	120	160	1.26×10^{-2}	55	2
1T-MoS_2	0.5 M H_2SO_4	100	207	N/A	40	3
Li-MoS_2/carbon fiber paper	0.5 M H_2SO_4	100	N/A	N/A	62	4
MoS_2/Au	0.5 M H_2SO_4	90	N/A	9.3×10^{-3}	69	5
MoO_3/MoS_2 nanowires	0.5 M H_2SO_4	150~200	240	N/A	50~60	6
Co-promoted MoS_2 film	1.0 M H_2SO_4	N/A	N/A	5.0×10^{-4}	43	7
MoS_2/RGO nanosheet hybrids	0.5 M H_2SO_4	140	N/A	N/A	41	8
MoS_2 nanosheet arrays/CFC	0.5 M H_2SO_4	N/A	224	N/A	58	9
Vertically aligned MoS_2 film	0.5 M H_2SO_4	N/A	N/A	2.2×10^{-3}	40	10
Ultrathin MoS_2 nanoplates	0.5 M H_2SO_4	90	N/A	N/A	53	11
MoS_2-carbon nanopapers	0.5 M H_2SO_4	N/A	80	N/A	41	12
MoS_2/graphene	0.5 M H_2SO_4	100	150	N/A	41	13
Vertically aligned MoS_2/CFC	0.5 M H_2SO_4	100	205	N/A	39	14
Mesoporous 1T –MoS_2	0.5 M H_2SO_4	N/A	154	1.58×10^{-2}	43	15
2H-MoS_2 with strained S vacancies	0.5 M H_2SO_4	N/A	170	N/A	60	16
MoS_2 (0 min)	0.5 M H_2SO_4	178	276	6.9×10^{-3}	96	This work
MoS_2 (30 min)	0.5 M H_2SO_4	84	192	6.0×10^{-2}	70	This work
MoS_2 (60 min)	0.5 M H_2SO_4	50	131	9.3×10^{-2}	64	This work
MoS_2 (90 min)	**0.5 M H_2SO_4**	**15**	**70**	**4.3×10^{-1}**	**36**	**This work**

Movies S1 and S2. Digital videos taken from (1) MoS_2/CFC and (2) MoS_2@Pt electrodes during their HER processes at a constant potential of -0.3 V vs. SAE. The more vigorous effervescence with the H_2 bubbles over MoS_2@Pt electrode directly illuminates that the surface Pt decoration enables MoS_2 with more promise for realistic HER application.